Documentation for the
Global Gridded Relative Deprivation Index (GRDI), Version 1

November 2022

Center for International Earth Science Information Network (CIESIN),
Columbia University

Abstract

The Global Gridded Relative Deprivation Index (GRDI), Version 1 (GRDIv1) data set characterizes the relative levels of multidimensional deprivation and poverty in each 30 arc-second (~1 km) pixel, where a value of 100 represents the highest level of deprivation and a value of 0 the lowest. GRDIv1 is built from sociodemographic and satellite data inputs that were spatially harmonized, indexed, and weighted into six main components to produce the final index raster. Inputs were selected from the best-available data that either continuously vary across space or have at least administrative level 1 (provincial/state) resolution, and which have global spatial coverage.

Data set citation: Center for International Earth Science Information Network (CIESIN), Columbia University. 2022. Global Gridded Relative Deprivation Index (GRDI), Version 1. Palisades, New York: NASA Socioeconomic Data and Applications Center (SEDAC). https://doi.org/10.7927/3xxe-ap97. Accessed DAY MONTH YEAR.

Suggested citation for this document: Center for International Earth Science Information Network (CIESIN), Columbia University. 2022. Documentation for the Global Gridded Relative Deprivation Index (GRDI), Version 1. Palisades, New York: NASA Socioeconomic Data and Applications Center (SEDAC). https://doi.org/10.7927/xwf1-k532. Accessed DAY MONTH YEAR.

We appreciate feedback regarding this data set, such as suggestions, discovery of errors, difficulties in using the data, and format preferences. Please contact:

NASA Socioeconomic Data and Applications Center (SEDAC)
Center for International Earth Science Information Network (CIESIN)
Columbia University
Phone: 1 (845) 365-8920
Email: ciesin.info@ciesin.columbia.edu

Documentation last revised November 16, 2022.

Contents

I.   Introduction

The Global Gridded Relative Deprivation Index (GRDI), Version 1 (GRDIv1) characterizes the levels of multidimensional deprivation and poverty for each 30 arc-second (~1 km) pixel in a raster image, where a value of 100 represents the highest level of deprivation and a value of 0 the lowest. GRDIv1 defines areas of relative deprivation using non-traditional inputs at a higher resolution than previously possible, and for the entire world. GRDIv1 defines areas of relative deprivation using relatively high-resolution data inputs for the entire world. The input data represent six dimensions of deprivation—child dependency ratios, infant mortality rates, a subnational human development index, building footprints per square kilometer, and nighttime lights (both current and recent changes). The resulting index value characterizes relative multidimensional deprivation across national and subnational boundaries. The GRDIv1 utilized the spatial indexing method Vulnerability Hotspot Mapping approach developed by CIESIN (CIESIN, 2015), where harmonized gridded data representing different facets of vulnerability are normalized into indicators and then combined into a final index. Similarly, the input components of GRDIv1 were converted into individual indicators on a 0-100 score, then aggregated and combined into the final index.

The first Sustainable Development Goal (SDG) in the United Nations (UN) 2030 Agenda seeks to end poverty of all forms everywhere by reaching the poorest of the poor, and to ensure progress for all population groups (the Leave No One Behind agenda). The aim is to achieve this globally at the highest disaggregated levels, including across geographic and governmental boundaries (UNDP, 2018; UNGA, 2015). Individual economic dimensions of income and wealth have traditionally measured poverty. For example, the World Bank defined the global extreme-poverty line as $1.90 USD income or below per day, which is based on the national poverty lines of the world's 15 poorest countries (World Bank, 2020). However, these indicators do not

2

entirely consider other non-financial forms of poverty that may be of equal importance. The concept of multidimensional poverty encompasses a more holistic view because it attempts to account for the lived experiences of people and the multiple deprivations they face in their daily lives beyond their incomes (OPHI, 2015a, 2015b; UNDP, 2020). UNDP and OPHI (2020) estimate that in 2018, 1.3 billion people, or 22% of the world's population, lived in multidimensional poverty, with half being under the age of 18.

GRDIv1 has six input components, or dimensions, that are combined to determine the degree of relative deprivation. First, the Child Dependency Ratio (CDR) is defined as the ratio between the populations of children (ages 0 to 14) to the working-age population (age 15 to 64) where a higher ratio implies a higher dependency on the working population (UN DESA, 2006). CDR is interpreted as a dimension where higher dependency ratios, generally associated with younger age structures, imply higher relative deprivation. Second, Infant Mortality Rates (IMR), defined as the number of deaths in children under 1 year of age per 1,000 live births in the same year, are a common indicator of population health (Reidpath and Allotey, 2003; Schell et al., 2007). Higher IMRs imply higher deprivation. Third, the Subnational Human Development Index (SHDI) attempts to assess human well-being through a combination of "three dimensions: Education, health, and standard of living[1] (Smits and Permanyer, 2019)". Lower SHDIs imply higher deprivation. Fourth, global rural populations are more likely to experience a higher degree of multidimensional poverty when compared to urban populations, other things being equal (Castañeda et al., 2018; Laborde Debucquet and Martin, 2018; Lee and Kind, 2021; UN DESA, 2021; UNDP and OPHI, 2020). Therefore, the ratio of built-up area to non-built up area (BUILT) is considered as a dimension where low values imply higher deprivation. The final two dimensions relate to the intensity of nighttime lights, which is closely associated with anthropogenic activities, economic output, and infrastructure development (Elvidge et al., 2007; Ghosh et al., 2013; Lu et al., 2021; Small et al., 2013). For the fifth component, the average intensity of nighttime lights for the year 2020 (Visible Infrared Imaging Radiometer Suite [VIIRS] Night Lights (VNL) 2020) is interpreted as a dimension where lower values imply higher deprivation. For the sixth component, the slope of a linear regression was calculated from annual VNL data between 2012 and 2020 (VNL slope) where higher values (increasing brightness) imply decreasing deprivation and lower values (decreasing brightness) imply increasing deprivation.

II.   Data and Methodology

Input data

GRDIv1 used nine input data sets to create the six components described above, along with one ancillary data set for alignment and resolution (Table 1). This latter data set, Gridded Population of the World, Version 4 (GPWv4): National Identifier Grid, Revision 11 (NIDv4.11) (CIESIN, 2018) provided the country ID and the spatial reference for geoprocessing tools, as well as Environment settings, including cell size, output coordinates (WGS84), snap raster, and extent.

---

[1] Standard of living is defined in the International Wealth Index (IWI) as an indicator of long-term socioeconomic position used to measure household wealth in Gross National Income (GNI) per capita (PPP, 2011 US$), and it is based on asset ownership, housing quality and access to public service (Smits and Steendijk, 2015).

Table 1: Information for input data sets: source, timeframe provided, frequency at which each input data observation was provided, format of the data set, and resolution.

Data Set	Data Source	Time Frame	Format	Resolution
Gridded Population of the World, Version 4 (GPWv4): National Identifier Grid, Revision 11 (NIDv4.11)	CIESIN, Columbia University	2010	Raster	30 arc-second (~1 km)
Gridded Population of the World, Version 4 (GPWv4): Basic Demographic Characteristics, Revision 11 (BDCv4.11)	CIESIN, Columbia University	2010	Shapefile	Best-available Admin unit
Global Subnational Infant Mortality Rates, Version 2.01 (IMRv2.01)	CIESIN, Columbia University	2015	Raster	30 arc-second (~1 km)
High-Resolution Settlement Layer (HRSL)	Facebook Connectivity Lab and CIESIN, Columbia University	2015	Shapefile	30 meters (~1 km)
CanadianBuildingFootprints, Version 1.1 (MS)	Microsoft	2019	Shapefile	N / A[2]
Gridded maps of building patterns throughout sub-Saharan Africa, Version 2.0 (ECOP)	Dooley et al., 2021. Ecopia	2020	Raster	3 arc-second (~100 m)
OpenStreetMap (OSM)	Geofabrik, 2018	Accessed 2021[1]	Shapefile	N / A[2]
Subnational Human Development Index (SHDI), Version 4.0	Global Data Lab	2018	Shapefile	Sub-national regions
Gridded global data sets for Gross Domestic Product (GDP) and Human Development Index (HDI) over 1990-2015, Version 2.0	Kummu, M. et al., 2020.	1990 - 2015	netCDF	5 arc-minute (~9.3 km)
Annual Visible Infrared Imaging Radiometer Suite [VIIRS] Nighttime Lights (VNL), Version 2.0	Elvidge et al., 2021. Earth Observatory Group (EOG)	2012 - 2020	Raster	15 arc-second (~500 m)

[1] OSM data are updated regularly; as a result, no temporal frame was given.
[2] Developed using satellite imagery and drawing polygon vectors that have no resolution.

The input data were harmonized into the six components using Esri ArcGIS geoprocessing and R (R Studio) tools, and eventually aggregated them into the final GRDIv1 data set. Individual inputs were as follows:

Component 1: The Child Dependency Ratio component (CDR) was calculated using data from the Gridded Population of the World, Version 4 (GPWv4): Basic Demographic Characteristics, Revision 11 (BDCv4.11) (2010) (CIESIN, 2018a). The BDCv4.11 is a gridded data set that was developed using shapefiles at the highest-level administrative units available for each country, which included Broad Age Group data for ages 0-14 (both sexes) and ages 15-64 (both sexes) used to calculate CDR. The CDR is calculated at the level of administrative (or census) units, and the result is applied to all grid cells within those units.

Component 2: Gridded Infant Mortality Rates (IMR) data came from the Global Subnational Infant Mortality Rates, Version 2.01 (IMRv2.01) (2015) downloaded from SEDAC (CIESIN,

2021). As with BDCv4.11, the underlying vital statistics reporting units vary in size, but are generally at a lower spatial resolution than BDCv4.11. Further information can be found in the data set documentation.

Component 3: The Subnational Human Development Index (SHDI), Version 4.0 shapefile from the Global Data Lab Subnational Human Development Index (Global Data Lab, 2020) was used. SHDIv4.0 provides data for 162 countries, or 1,779 sub-national regions. Please refer to the SHDI documentation for a list of countries and regions.

The Gridded global data sets for Gross Domestic Product (GDP) and Human Development Index over 1990-2015, Version 2.0 (HDIv2) were used to gap-fill grid cells that were missing SHDI data. Specifically, the 'HDI_1990_2015_v2.nc', February 13, 2020 release file (Kummu et al., 2018, 2020).

Component 4: The ratio of built-up area to non-built up area (BUILT) component was derived from three data sets, depending on the region. The primary input was the High-Resolution Settlement Layer (HRSL) (Facebook Connectivity Lab and CIESIN, 2016). The HRSL layer provided shapefile polygons for 140 countries that represent the areas that have been settled at a 30 m resolution. For more information on which countries are available, please refer to the HRSL documentation (Facebook Connectivity Lab and CIESIN, 2016). The gap-filled countries and regions with ancillary data are listed below (Appendix 3).

Canada's building footprints were acquired from Microsoft's CanadianBuildingFootprints Version 1.1 (MS), June 13, 2019 release (Microsoft, 2019). Microsoft provided GeoJSON features that represent building footprints.

Building footprints for Ethiopia, Somalia, Sudan, Zambia, and Zimbabwe were collected from Gridded maps of building patterns throughout sub-Saharan Africa, Version 2.0 (ECOP) (Dooley et al., 2021) available from WorldPop, https://data.worldpop.org/repo/wopr/_MULT/buildings/v2.0/. WorldPop provided 100 m resolution rasters for each country. The rasters used were the XXX_buildings_v1_1_total_area.tif, where XXX is a particular country. These rasters contain a grid-cell-level "sum of the building areas for all buildings whose centroid falls inside a grid cell in m^2". Note: Total building area could exceed the area of a grid cell if the centroid of a large building falls within the grid cell (Dooley et al., 2021)."

Finally, Building footprints were downloaded from Geofabrik's OpenStreetMap (OSM) project (Geofabrik, 2018), which provided polygons that represent building footprints for the following countries/regions: Afghanistan, American Oceania, Australia, Azerbaijan, Brazil, China, Cuba, Cyprus, Dominican Republic, Greenland, Hungary, Iran, Kosovo, Libya, Montenegro, Morocco, Myanmar, North Korea, Norway (Svalbard), Poland, Russia, Serbia, Slovakia, Syria, Ukraine, U.S. (Alaska), Venezuela, and Yemen.

Components 5 and 6: The Visible Infrared Imaging Radiometer Suite [VIIRS] Nighttime Lights, Version 2.0 (VNLv2) data from the Earth Observatory Group (EOG) at the Payne Institute (Elvidge et al., 2021), in particular, the "average_masked" rasters—with background,

biomass burning, and aurora zeroed out— from 2012 to 2020 were downloaded. EOG provided two options for the 2012 VLN due to data availability, April 2012 – December 2012 or April 2012 - March 2013, of which the latter was selected.

Methods

A global Fishnet feature class was created in Esri ArcGIS Pro using the NIDv4.11 raster as a reference for grid cell size, output coordinates (WGS84), snap raster, and extent. Each grid cell in the Fishnet was assigned a unique ID, referred to as 'gridcode'. A python multiprocessing script was used to divide the Fishnet into 10-degree-tiled Fishnet rasters. The type of input data provided determined the processing method in order to spatially harmonize the data (Figure 1).
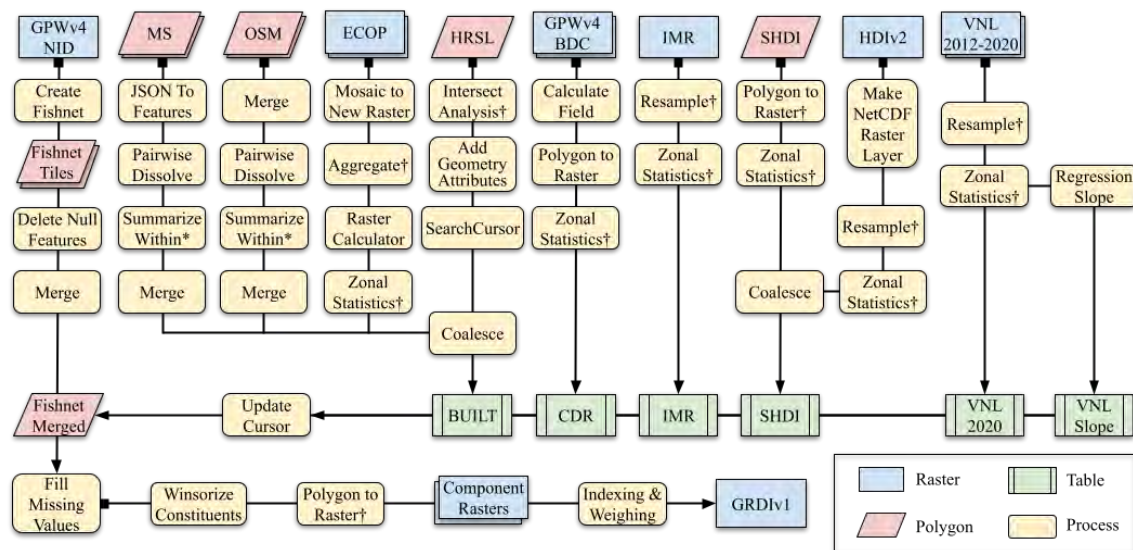
Figure 1: Workflow process of GRDIv1 from top to bottom. Rasters (blue) and shapefiles (red) at the top of this figure were processed with specific geoprocessing tools (yellow) according to the type of input data provided. The resulting input components (green) were aggregated to create the GRDIv1 product. Note: Processing tools that used the tiled rasters are denoted with a dagger (†), and the processing tools that used the tiled Fishnet feature classes are denoted with an asterisk (*); all processing tools used NIDv4.11 for grid cell size and spatial reference.

CDR
The CDRs were calculated using Equation 1 (UN DESA, 2006) in tandem with the broad age groups from the BDCv4.11 rasters,

$$CDR = \text{<Population\_0-14\_Raster>} / \text{<Population\_15-64\_Raster>} \tag{1}$$

where the dependent population of ages 0-14, is divided by the working-age population of ages 15-64. The CDR was calculated by creating a new data field in each shapefile and using the Calculate Field and Equation 1. For instances where the CDR could not be calculated due to zero values, it was determined that, independently of other conditions, that if there are zero children recorded or if the total population is zero, then the CDR was set to 0. The Polygon to Raster tool converted each shapefile to a 100m-resolution raster. The grid cell size was set to $8.3333e^{-4}$, and the NIDv4.11 raster was set as the coordinate system and snapping environments. The Mosaic to New Raster combined all of the country/region CDR rasters using Mean as the Mosaic Operator

that determines the value of overlapping areas. The CDR raster was exported as Comma Separated Values (CSV) files using the Zonal Statistics as Table tool with the tiled Fishnet rasters as the zone field in order to harmonize the CDR with the other GRDIv1 inputs.

IMR

The IMR raster was aligned to the Fishnet using the Resample tool in ArcGIS Pro with a Nearest Neighbor method; the NIDv4.11 raster provided the grid cell size and spatial reference. The Zonal Statistics as Table tool was used with the NIDv4.11 raster as the summary area so that each grid cell was given a gridcode and an IMR value in CSV format.

SHDI

The SHDI shapefile was converted to a raster using the Polygon to Raster tool in ArcGIS Pro with a "Maximum area" grid cell assignment type. The Zonal Statistics as Table tool was used to export the SHDI values and the corresponding gridcode in CSV format. Again, the NIDv4.11 raster was used as a reference for grid cell size, output coordinates, and snap.

The HDIv2 NetCDF file was converted to a raster using the Make NetCDF Raster Layer tool. The resulting raster was aligned and its resolution increased using the Resample tool with the NIDv4.11 raster as a reference for grid cell size, output coordinates, and snap. The Zonal Statistics tool was used as described in the SHDI section above.

The CSVs were imported into R as Data Frames. We performed a full_join of the two input data sets using the gridcode as the joining variable and created a new dataframe. A new Data Frame column coalesced the data sets where the row was first populated by SHDI, then, if null, by HDIv2. The results were exported in CSV format.

BUILT

The input HSRL polygons were combined with the Fishnet using the Intersect Analysis tool, splitting the HRSL polygons that crossed the Fishnet polygons. The Add Geometry Attributes tool was used to calculate the areas, in km^2, for each HRSL polygon. A data dictionary was generated where each polygon was represented as a row with the overlapping gridcode and the area of the polygon. The SearchCursor tool was used to iterate through the dictionary to sum up the areas that had identical gridcodes. The total HRSL areas and corresponding gridcode of the dictionary were exported as CSV files.

The MS GeoJSON features were converted to feature classes using the JSON To Features (Conversion) tool. The Pairwise Dissolve tool was used to remove any overlap from the polygons. The Summarize Within tool was used to summarize the areas of the polygons, in km^2, that fell within each gridcode cell of the Fishnet. This process generated tiled feature classes. The Merge tool was used to combine the tiles into a single gridded feature class. A CSV file was exported from the resulting MS feature class.

The Mosaic To New Raster tool in ArcGIS Pro was used to join the ECOP rasters into one with a "Maximum" mosaic operator that chooses the maximum value if multiple values overlap. To keep the integrity of the counts and area of ECOP while aligning with the NIDv4.11 raster, the Aggregate tool was used on the raster using a grid cell factor of 10 and a "SUM" Aggregation technique; the raster extent was allowed to expand if needed, and the No Data values were

7

ignored; the NIDv4.11 raster was used as the snap raster. The Raster Calculator tool was then used to convert the m^2 values to km^2 using Equation 2:

$$x\ km^2 = x\ m^2 \cdot \frac{1.0e^{-6}\ km^2}{1 m^2}$$

(2)

where *x* is the value of the corresponding pixel. The Zonal Statistics as Table tool produced a CSV file with the aggregated ECOP value and corresponding gridcode of the Fishnet.

The OSM shapefiles were provided by region, which sometimes had overlaps of buildings; as a result, the shapefiles were merged into one feature class using the Merge tool. The Pairwise Dissolve tool was then used to create a single feature class without overlap. The Summarize Within tool was used to summarize the areas of the polygons, in km^2, that fell within each fishnet cell. This process generated tiled feature classes. The Merge tool was used to combine the tiles into a single gridded OSM feature class. The Table to Table tool was used to export a CSV file from the resulting OSM feature class.

The CSVs of HRSL, ECOP, MS, and OSM were merged to make the BUILT component. R was used to perform a full_join of the four input data sets using the gridcode as the joining variable and created a new dataframe. A new column coalesced the four data sets where the row was first populated by HRSL, then, if null, by ECOP, then, if null, by MS, and then, if still null, by OSM. The rows that had No Data in the BUILT column were dropped using drop_na() in R. A complete BUILT.CSV file was exported.

VNL 2020
The VNLv2 2012-2020 annual rasters were resampled to a 30 arc-second resolution using a bilinear method in the ArcGIS Pro Resample tool, which averages (weighted for distance) the values of the nearest four pixels; the NIDv4.11 raster was used as a reference for grid cell size, output coordinates, snap raster, and extent. VNL data carries some negative values for calibration purposes and for time series comparisons, so it is sometimes recommended to set a bottom limit (Chen and Nordhaus, 2015; Elvidge et al., 2021); thus, VNL values that were < 0.01 were set to 0. The resampled VNL rasters from 2012-2020 were exported as CSV files by using the Zonal Statistics as Table tool and setting the gridcode raster as the zone field. VNL 2020 was used as a GRDI input.

VNL Slope
The VNL 2012-2020 data in CSV format was used to calculate the VNL Slope for each Fishnet grid cell using a linear regression function created by the lm() function in R, which returns a summary object with statistical information of the function, including the slope for each grid cell (Equation 3),

$$lm\_Summary <-\ lm(y \sim x)$$

(3)

$$VNL\_slope <- lm\_Summary\$coefficients[2]$$

where lm_Summary is the object generated by the lm() function, y is a list of the dependent variables, in this case the VNL values, x is a list of the independent variable, in this case the corresponding year of the VNL value, VNL_slope is the resulting slope value, and 2 is the position of the slope value in the summary object. The output CSV contained the slope value of the linear regression and the gridcode for each Fishnet grid cell.

Creation of the GRDI Index from the Six Components
The resulting components of GRDIv1—BUILT, CDR, IMR, SHDI, VNL 2020, and VNL slope were bounded—by importing the CSV files into R and performing a full_join, which matched each row in all of the CSVs by the gridcode. The values were rounded to the 6th decimal number to limit data artifacts of the floating-point format used. The data frame was tiled and exported into CSVs according to the Fishnet tile number. A Python script joined the tiled CSVs to the corresponding tiled Fishnet features by matching the gridcode. The grid cells in the resulting tiled Fishnet features that had No Data in the BUILT field were removed. The tiled Fishnet features were merged into a single feature class.

No Data values in all input components, except BUILT, were filled using the Fill Missing Values tool in ArcGIS Pro, using the 8-neighbors `Average` Fill method and using the gridcode as the unique ID. This tool outputs a separate 'FILLED' feature, which was joined to the GRDIv1 Fishnet using the gridcode as the joining field; the missing values for each component's field were selected and replaced by the 'FILLED' values using the Select Features and Raster Calculator tools, respectively. A raster that counts the number of components that were filled using this process per grid cell is available for download. Once the missing values were filled, a raster for each of the six input components was generated.

An indexing method was applied according to the Vulnerability Hotspot Mapping method developed by CIESIN as the following: The SearchCursor tool was used to create a list of all values for each component. The numpy.quantile python function was used to determine the 5% and 95% quantiles for each component. The UpdateCursor tool was used to iterate through the Fishnet and update the values if they are below or above the quantiles, accordingly. The winsorized input components were then indexed from 0-100 according to how the input is interpreted, i.e. a low value in BUILT and a high value in CDR both imply high deprivation. Each component had a weight applied according to the original data set resolution where a coarser resolution was assigned a lower weight (Table 2).

Table 2: The resulting components of GRDIv1, how they are interpreted in the first indexing process, and the subsequent weight that was applied once the components are aggregated.

Data	BUILT	CDR	IMR	SHDI	VNL 2020	VNL Slope
Values that imply high vulnerability	Low	High	High	Low	Low	Low
Weight	0.2	0.2	0.1	0.1	0.2	0.2

Once the weights were applied, the weighted indices of all input components were summed for each Fishnet grid cell, divided by six (the number of components) and exported as a raster, which

again was indexed from 0-100 into the final GRDIv1 raster using the Raster Calculator, where 100 represents the highest deprivation level and 0 the lowest (Figure 2).
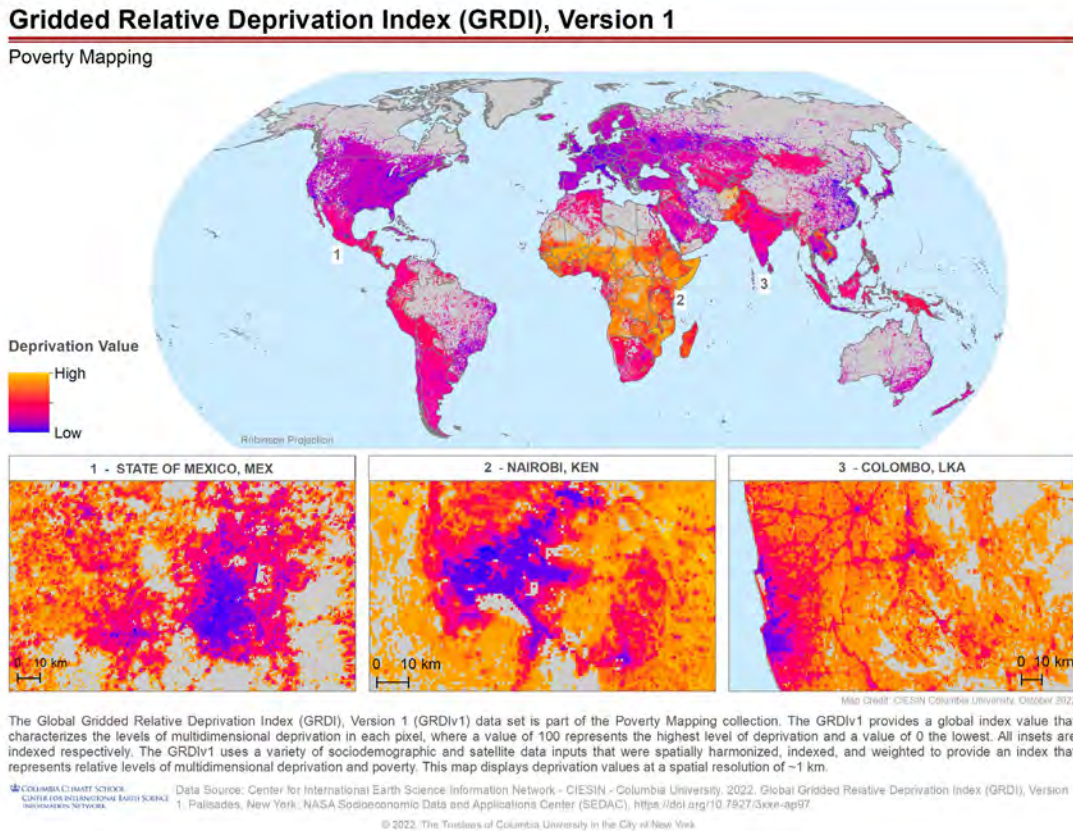
Figure 2: A projection of the Global Gridded Relative Deprivation Index (GRDI), Version 1. The GRDIv1 data set provides a global index value that seeks to characterize the levels of multidimensional deprivation and wellbeing in each pixel, where a value of 100 represents the highest level of deprivation and a value of 0 the lowest. All insets are indexed dynamically to show the local relativity of GRDIv1.

III. Data Set Description(s)

The GRDIv1 raster data set represents the degree of relative deprivation at a 30 arc-second (~1 km) spatial resolution. The 32-bit floating point values range from 0.00 to 100.00, with 0 representing the lowest deprivation level and 100 representing the highest. The areas with No Data values are a result of there not being any building footprints present in the original input data.

Data set web page:
SEDAC URL: https://sedac.ciesin.columbia.edu/data/set/povmap-grdi-v1
Permanent URL: https://doi.org/10.7927/xwf1-k532

Data set format:
The data are available in GeoTIFF format at ~1 km resolution. The downloadables are compressed zip files containing: 1) GeoTIFFs, 2) Readme.TXT file, and 3) PDF Documentation. The GRDIv1 GeoTIFFs are:

- povmap-grdi-v1.tif - Global Gridded Relative Deprivation Index (GRDI), Version 1
- povmap-grdi-v1_BUILT.tif - BUILT Component, indexed 0 to 100
- povmap-grdi-v1_CDR.tif - Child Dependency Ratio (CDR) Component, indexed 0 to 100
- povmap-grdi-v1_IMR.tif - Infant Mortality Rates (IMR) Component, indexed 0 to 100
- povmap-grdi-v1_SHDI.tif - Subnational Human Development Index (SHDI) Component, indexed 0 to 100
- povmap-grdi-v1_VNL-2020.tif - VIIRS Nighttime Lights (VNL) 2020 Component, indexed 0 to 100
- povmap-grdi-v1_VNL-slope.tif - VIIRS Nighttime Lights (VNL) Slope Component, indexed 0 to 100
- povmap-grdi-v1_FilledMissingValues-Count.tif - Raster showing count of components that were filled-in per grid cell using the Fill Missing Values tool

Data set downloads:
- povmap-grdi-v1-geotiff.zip - contains all GeoTIFFs listed above
- povmap-grdi-v1-grdiv1-geotiff.zip - contains the final GRDIv1 GeoTIFF only
- povmap-grdi-v1-built-geotiff.zip - contains the GRDIv1 BUILT GeoTIFF only
- povmap-grdi-v1-cdr-geotiff.zip - contains the GRDIv1 CDR GeoTIFF only
- povmap-grdi-v1-imr-geotiff.zip - contains the GRDIv1 IMR GeoTIFF only
- povmap-grdi-v1-shdi-geotiff.zip - contains the GRDIv1 SHDI GeoTIFF only.
- povmap-grdi-v1-vnl-2020-geotiff.zip - contains the GRDIv1 VNL_2020 GeoTIFF only
- povmap-grdi-v1-vnl-slope-geotiff.zip - contains the GRDIv1 VNL_slope GeoTIFF only
- povmap-grdi-v1-filledmissingvalues-count-geotiff.zip - contains the GRDIv1 FilledMissingValues-Count GeoTIFF only

IV. How to Use the Data

The raster data in GeoTIFF format can be used directly in mapping and geospatial analysis in tandem with other spatial data sets.

V. Potential Use Cases

The GRDIv1 data is of use to Earth scientists, demographers, policy makers, government planners and leaders, NGOs (including humanitarian and development actors), climate adaptation planners, emergency responders, and the general public. GRDIv1 has several potential uses that focus on identifying relative poverty and deprivation at a higher resolution, and with

more inputs, than the current multidimensional poverty data sets available. One use case is the integration with Earth observation data, including hazards and climate impacts data, to identify hotspots of vulnerability and risk. This data set is of use to humanitarian organizations in order to target resources locally in the aftermath of disasters. The GRDIv1 has a number of development-related applications, including pursuit of the 2030 Agenda on Sustainable Development. Data from SEDAC incorporates open map services for use in its own and third party online mapping tools.

VI.   Limitations

GRDIv1 uses the latest available releases of a wide range of input data sets from a variety of sources. These input data are developed using varying methods and spatiotemporal resolutions. As a result, GRDIv1 is an index that represents relative levels of deprivation, rather than absolute levels of deprivation. Furthermore, owing to the use of built-up areas and nighttime lights, the GRDIv1 may not fully capture intra-urban differentials in deprivation.

GRDIv1 data is available in 228 countries or regions. Building footprints for twenty-two countries and regions identified by NIDv4.11 were not available within the data sources used; therefore, they are omitted from GRDIv1 (Appendix 4).

The BUILT layer is a composition of three different data sets with unique definitions of the building footprint (please see above for each definition). Where data are gap-filled from sources other than the High Resolution Settlement Layer (Appendix 3), the definitions of "built up areas" applied in each source (described on page 5) will affect relative deprivation layers since the assumption is that more built up areas are less deprived. Furthermore, the relationship between built up area and deprivation is debatable in different contexts. For example, as noted above, intra-urban poverty is heterogeneous, so rapid and unplanned urbanization may increase the urban population that lives with high degrees of deprivation and poverty, particularly in developing countries (Cardona et al., 2012; Ravallion et al., 2007; Rignall and Atia, 2017). This suggests that certain kinds of built up areas (e.g., informal settlements) may have high degrees of relative deprivation compared to others (e.g., more formal settlements and central business districts). In the developed world, on the other hand, the correlation between living in urban built up areas and wellbeing is not so straightforward, as can be seen in the economic contrasts between wealthy suburbs and inner-city neighborhoods with high poverty rates. Therefore, while at a global level, the relationship between built up areas and relative deprivation may be inversely linear, in certain contexts the relationship may break down.

Some of the processing tools used in GRDIv1 generated No Data values. For example, VNL Slope results as No Data if all of the input data points were 0, thus, the VNL Slope in these cases was assumed to be 0. Calculating CDR with zero value inputs returned an error and were considered as No Data. IMR assigned some grid cells a water value despite BUILT identifying a building in that location, thus, were considered as No Data. The SHDI polygon did not overlay some of the grid cells, particularly along the coasts and were recorded as No Data. Any missing

data points were filled using ancillary data mentioned in the documentation above, and if still null, filled in using an average of the nearest eight spatial neighbors.

VII. Acknowledgments

VIII. Disclaimer

CIESIN follows procedures designed to ensure that data disseminated by CIESIN are of reasonable quality. If, despite these procedures, users encounter apparent errors or misstatements in the data, they should contact SEDAC User Services at ciesin.info@ciesin.columbia.edu. Neither CIESIN nor NASA verifies or guarantees the accuracy, reliability, or completeness of any data provided. CIESIN provides this data without warranty of any kind whatsoever, either expressed or implied. CIESIN shall not be liable for incidental, consequential, or special damages arising out of the use of any data provided by CIESIN.

IX. Use Constraints

X. Recommended Citation(s)

Data set(s):

Center for International Earth Science Information Network (CIESIN), Columbia University. 2022. Global Gridded Relative Deprivation Index (GRDI), Version 1. Palisades, New York: NASA Socioeconomic Data and Applications Center (SEDAC). https://doi.org/10.7927/3xxe-ap97. Accessed DAY MONTH YEAR.

XI.   Source Code

No source code is provided.

XII.   References

Cardona, O.-D., M. K. van Aalst, J. Birkmann, M. Fordham, G. McGregor, R. Perez, R. S. Pulwarty, E. L. F. Schipper, B. T. Sinh, H. Décamps, M. Keim, I. Davis, K. L. Ebi, A. Lavell, R. Mechler, V. Murray, M. Pelling, J. Pohl, A.-O. Smith, and F. Thomalla. 2012. Determinants of Risk: Exposure and Vulnerability. In C. B. Field, V. Barros, T. F. Stocker, and Q. Dahe (Eds.), *Managing the Risks of Extreme Events and Disasters to Advance Climate Change Adaptation* (pp. 65–108). Cambridge University Press. https://doi.org/10.1017/CBO9781139177245.005.

Castañeda, A., D. Doan, D. Newhouse, M. C. Nguyen, H. Uematsu, and J. P. Azevedo. 2018. A new profile of the global poor. *World Development*, 101(C), 250–267. https://econpapers.repec.org/article/eeewdevel/v_3a101_3ay_3a2018_3ai_3ac_3ap_3a250-267.htm, https://openknowledge.worldbank.org/handle/10986/29225.

Center for International Earth Science Information Network (CIESIN), Columbia University. 2015. A Step-by-Step Guide to Vulnerability Hotspots Mapping: Implementing the Spatial Index Approach. https://ciesin.columbia.edu/documents/vmapping_guide.pdf.

Center for International Earth Science Information Network (CIESIN), Columbia University. 2018a. Documentation for the Gridded Population of the World, Version 4 (GPWv4), Revision 11 Data Sets. https://doi.org/10.7927/H45Q4T5F.

Center for International Earth Science Information Network (CIESIN), Columbia University. 2018b. Gridded Population of the World, Version 4 (GPWv4): Basic Demographic Characteristics, Revision 11. Palisades, NY: NASA Socioeconomic Data and Applications Center (SEDAC). https://doi.org/10.7927/H46M34XX.

Center for International Earth Science Information Network (CIESIN), Columbia University. 2018c. Gridded Population of the World, Version 4 (GPWv4): National Identifier Grid, Revision 11. Palisades, NY: NASA Socioeconomic Data and Applications Center (SEDAC). https://doi.org/10.7927/H4TD9VDP.

Center for International Earth Science Information Network (CIESIN), Columbia University. 2021. Global Subnational Infant Mortality Rates, Version 2.01. Palisades, NY: NASA Socioeconomic Data and Applications Center (SEDAC). https://doi.org/10.7927/0GDN-6Y33.

Chen, X., and W. Nordhaus. 2015. A test of the new VIIRS Lights Data Set: Population and economic output in Africa. *Remote Sensing*, 7(4), 4937–4947. https://doi.org/10.3390/rs70404937.

Dooley, C., D. Leasure, G. Boo, and A. Tatem. 2021. Gridded maps of building patterns

throughout sub-Saharan Africa, version 2.0. University of Southampton. Southampton, UK. Source of building footprints "Ecopia Vector Maps Powered by Maxar Satellite Imagery"© 2020/2021. https://eprints.soton.ac.uk/442215/, https://doi.org/10.5258/SOTON/WP00677.

Elvidge, C. D., J. Safran, B. Tuttle, P. Sutton, P. Cinzano, D. Pettit, J. Arvesen, and C. Small. 2007. Potential for global mapping of development via a nightsat mission. *GeoJournal*, 69(1), 45–53. https://doi.org/10.1007/s10708-007-9104-x.

Elvidge, C. D., M. Zhizhin, Y. Ghosh, F.-C. Hsu, and J. Taneja. 2021. Annual time series of global VIIRS nighttime lights derived from monthly averages: 2012 to 2019. *Remote Sensing*, 13(5), 922. https://doi.org/10.3390/rs13050922.

Facebook Connectivity Lab, and Center for International Earth Science Information Network (CIESIN), Columbia University. 2016. High Resolution Settlement Layer (HRSL). https://www.ciesin.columbia.edu/data/hrsl/.

Geofabrik. 2018. OpenStreetMap Data Extracts. http://download.geofabrik.de/.
Ghosh, T., S. J. Anderson, C. D. Elvidge, and P. Sutton. 2013. Using nighttime satellite imagery as a proxy measure of human well-being. *Sustainability*, 5(12), 4988–5019. https://doi.org/10.3390/su5124988.

Global Data Lab. 2020. GDL Code & Shapefiles. Human Development Indices. https://globaldatalab.org/shdi/shapefiles/.

Kummu, M., M. Taka, and J. H. A. Guillaume. 2018. Gridded global datasets for Gross Domestic Product and Human Development Index over 1990–2015. *Scientific Data*, 5(1), 180004. https://doi.org/10.1038/sdata.2018.4.

Kummu, M., M. Taka, and J. H. A. Guillaume. 2020. Data from: Gridded global datasets for Gross Domestic Product and Human Development Index over 1990-2015 (Version 2, p. 481877286 bytes). Dryad. https://doi.org/10.5061/DRYAD.DK1J0.

Laborde Debucquet, D., and W. Martin. 2018. Implications of the global growth slowdown for rural poverty. *Agricultural Economics*, 49(3), 325–338. https://doi.org/10.1111/agec.12419.

Lee, Y. F., and M. Kind. 2021. Reducing poverty and inequality in rural areas: Key to inclusive development. https://www.un.org/development/desa/dspd/2021/05/reducing-poverty/.

Lu, D., Y. Wang, Q. Yang, K. Su, H. Zhang, and Y. Li. 2021. Modeling spatiotemporal population changes by integrating DMSP-OLS and NPP-VIIRS nighttime light data in Chongqing, China. *Remote Sensing*, 13(2), 284. https://doi.org/10.3390/rs13020284.

Microsoft. 2019. CanadianBuildingFootprints (1.1) [Computer software]. Microsoft. https://github.com/microsoft/CanadianBuildingFootprints.

OPHI. 2015a. Global Multidimensional Poverty Index. https://ophi.org.uk/multidimensional-

15

poverty-index/.

OPHI. 2015b. Policy – A Multidimensional Approach.
https://ophi.org.uk/policy/multidimensional-poverty-index/.

Ravallion, M., S. Chen, and P. Sangraula. 2007. New evidence on the urbanization of global poverty. *Population and Development Review*, 33(4), 667–701. https://doi.org/10.1111/j.1728-4457.2007.00193.x.

Reidpath, D. D., and P. Allotey. 2003. Infant mortality rate as an indicator of population health. *Journal of Epidemiology and Community Health*, 57(5), 344–346. https://doi.org/10.1136/jech.57.5.344.

Rignall, K., and M. Atia. 2017. The global rural: Relational geographies of poverty and uneven development. *Geography Compass*, 11(7), e12322. https://doi.org/10.1111/gec3.12322.

Schell, C. O., M. Reilly, H. Rosling, S. Peterson, and A. M. Ekström. 2007. Socioeconomic determinants of infant mortality: A worldwide study of 152 low-, middle-, and high-income countries. *Scandinavian Journal of Public Health*, 35(3), 288–297. https://doi.org/10.1080/14034940600979171.

Small, C., C. D. Elvidge, and K. Baugh. 2013. Mapping urban structure and spatial connectivity with VIIRS and OLS night light imagery. *Joint Urban Remote Sensing Event* 2013, 230–233. https://doi.org/10.1109/JURSE.2013.6550707.

Smits, J., and I. Permanyer. 2019. The Subnational Human Development Database. *Scientific Data*, 6(1), 190038. https://doi.org/10.1038/sdata.2019.38.

Smits, J., and R. Steendijk. 2015. The International Wealth Index (IWI). *Social Indicators Research*, 122(1), 65–85. https://doi.org/10.1007/s11205-014-0683-x.

UN Department of Economic and Social Affairs (DESA). 2006. Dependency Ratio. https://www.un.org/esa/sustdev/natlinfo/indicators/methodology_sheets/demographics/dependency_ratio.pdf.

UN Department of Economic and Social Affairs (DESA). 2021. World Social Report 2021: Reconsidering Rural Development. https://www.un.org/development/desa/dspd/world-social-report/2021-2.html.

UN Development Programme (UNDP). 2018. *What Does it Mean to Leave No One Behind: A UNDP Discussion Paper and Framework for Implementation* (29pp.). Bureau for Policy and Programme Support. https://www.undp.org/publications/what-does-it-mean-leave-no-one-behind.

UN Development Programme (UNDP). 2020. *Human Development Report 2020: The Next Frontier: Human Development and the Anthropocene*. New York.

16

https://hdr.undp.org/content/human-development-report-2020?utm_source=EN&utm_medium=GSR&utm_content=US_UNDP_PaidSearch_Brand_English&utm_campaign=CENTRAL&c_src=CENTRAL&c_src2=GSR&gclid=CjwKCAjwvsqZBhAlEiwAqAHElcMvC1mgo-flEeUSeY4OypOzK-MpKtZCn6z2vtxPaX7uyoT_TdU4oBoC7dMQAvD_BwE.

UN Development Programme (UNDP) and OPHI. 2020. *Global Multidimensional Poverty Index 2020—Charting Pathways Out of Multidimensional Poverty: Achieving the SDGs.* https://hdr.undp.org/content/2020-global-multidimensional-poverty-index-mpi?utm_source=EN&utm_medium=GSR&utm_content=US_UNDP_PaidSearch_Brand_English&utm_campaign=CENTRAL&c_src=CENTRAL&c_src2=GSR&gclid=CjwKCAjwvsqZBhAlEiwAqAHElV3dFJACpXE9ZKPBfp5h5pqNs7I6CvpeTluouYvZj8-QWw8jlE4pdRoCxwYQAvD_BwE.

UN General Assembly (UNGA). 2015. *Transforming our World: The 2030 Agenda for Sustainable Development* (A/RES/70/1). https://sdgs.un.org/2030agenda.

World Bank. 2020. *Poverty and Shared Prosperity 2020: Reversals of Fortune – Frequently Asked Questions*. World Bank. https://www.worldbank.org/en/research/brief/poverty-and-shared-prosperity-2020-reversals-of-fortune-frequently-asked-questions.

XIII. Documentation Copyright and License

Appendix 1. Data Revision History

No revisions have been made to this data set.

Appendix 2. Contributing Authors & Documentation Revision History

Revision Date	ORCID	Contributors	Revisions
November 16, 2022	0000-0002-8875-4864 0000-0002-9168-7172	Juan F. Martinez, Alex de Sherbinin, Susana Adamo, Elisabeth Sydor	This document is the 1st instance of documentation.

Appendix 3. Countries/Regions Using Ancillary Data in BUILT Component

Country/Region	Source
Afghanistan	Geofabrik, 2018
American Oceania	Geofabrik, 2018
Australia	Geofabrik, 2018
Azerbaijan	Geofabrik, 2018
Brazil	Geofabrik, 2018
Canada	Microsoft, 2019
China	Geofabrik, 2018
Cuba	Geofabrik, 2018
Cyprus	Geofabrik, 2018
Dominican Republic	Geofabrik, 2018
Ethiopia	Dooley et al., 2021
Greenland	Geofabrik, 2018
Hungary	Geofabrik, 2018
Iran	Geofabrik, 2018
Kosovo	Geofabrik, 2018
Libya	Geofabrik, 2018
Montenegro	Geofabrik, 2018
Morocco	Geofabrik, 2018
Myanmar	Geofabrik, 2018
North Korea	Geofabrik, 2018
Norway (Svalbard)	Geofabrik, 2018
Poland	Geofabrik, 2018
Russia	Geofabrik, 2018
Serbia	Geofabrik, 2018
Slovakia	Geofabrik, 2018
Somalia	Dooley et al., 2021
Sudan	Dooley et al., 2021
Syria	Geofabrik, 2018
Ukraine	Geofabrik, 2018

U.S. (Alaska)	Geofabrik, 2018
Venezuela	Geofabrik, 2018
Yemen	Geofabrik, 2018
Zambia	Dooley et al., 2021
Zimbabwe	Dooley et al., 2021

Appendix 4. Countries/Regions Omitted from GRDIv1

Country/Region
Aland Islands
Andorra
Bermuda
Bonaire, Sint Eustatius and Saba
Bouvet Island (Uninhabited)
British Indian Ocean Territory (Military personnel only)
Cook Islands
Curacao
Falkland Islands
French Southern and Antarctic Lands
Gibraltar
Niue
Papahānaumokuākea Marine National Monument (Uninhabited)
Saint Barthélemy
Saint Helena, Ascension and Tristan da Cunha
Sint Maarten
South Georgia and the South Sandwich Islands
Spratly Islands (Philippines)
The Bailiwick of Jersey
The Collectivity of Saint-Martin
The Overseas Collectivity of Saint-Pierre and Miquelon
Tokelau